

# Chemical Science

Accepted Manuscript

This article can be cited before page numbers have been issued, to do this please use: S. Dutta, S. Tripathy, S. Bej, S. Parvin, B. Jana, C. Patra and A. Das, *Chem. Sci.*, 2025, DOI: 10.1039/D5SC03783B.



This is an Accepted Manuscript, which has been through the Royal Society of Chemistry peer review process and has been accepted for publication.

Accepted Manuscripts are published online shortly after acceptance, before technical editing, formatting and proof reading. Using this free service, authors can make their results available to the community, in citable form, before we publish the edited article. We will replace this Accepted Manuscript with the edited and formatted Advance Article as soon as it is available.

You can find more information about Accepted Manuscripts in the [Information for Authors](#).

Please note that technical editing may introduce minor changes to the text and/or graphics, which may alter content. The journal's standard [Terms & Conditions](#) and the [Ethical guidelines](#) still apply. In no event shall the Royal Society of Chemistry be held responsible for any errors or omissions in this Accepted Manuscript or any consequences arising from the use of any information it contains.

# Esterase-induced release of a theranostic prodrug in lysosome for improved therapeutic efficacy and lower systemic toxicity

Sourav Dutta,<sup>#,a</sup> Sanchita Tripathy,<sup>#,b,c</sup> Somnath Bej,<sup>#,a</sup> Sabana Parvin,<sup>a</sup> Batakrishna Jana,<sup>\*,a,d</sup> Chitta Ranjan Patra,<sup>\*,b,c</sup> Amitava Das<sup>\*,a</sup>

<sup>a</sup>Department of Chemical Sciences and Centre for Advanced Functional Material  
Indian Institute of Science Education and Research (IISER) Kolkata Mohanpur 741246, India

<sup>b</sup>Department of Applied Biology, CSIR-Indian Institute of Chemical Technology, Uppal Road,  
Tarnaka, Hyderabad – 500007, Telangana State, India

<sup>c</sup>Academy of Scientific and Innovative Research (AcSIR), Ghaziabad-201002, India

<sup>d</sup>Department of Chemistry, School of Basic and Applied Sciences, Adamas University,  
Jagannathpur, Kolkata-700126

<sup>#</sup>Authors contributed equally to this work.

Corresponding author email: [batakrishna.jana1@adamasuniversity.ac.in](mailto:batakrishna.jana1@adamasuniversity.ac.in), [crpatra@iict.res.in](mailto:crpatra@iict.res.in), [amitava@iiserkol.ac.in](mailto:amitava@iiserkol.ac.in)

## Abstract

5-Fluorouracil (5-FU) is the third most used chemotherapeutic agent. Despite being a frontline drug, it inhibits thymidylate synthase in malignant and non-malignant cells, which adds to its severe systemic toxicity. To address this, a new physiologically benign theranostic prodrug of 5-FU, named PD, has been developed by covalently linking 5-FU with a fluorophore and a lysosome-targeting morpholine moiety through an ester functionality. Esterase (Est), being overexpressed in various cancer cells such as human glioblastoma (U87) cells, human ovarian cancer (SKOV-3), induces cleavage of the ester linkage and results in a sustained release of 5-Fluorouracil-1-acetic acid (FUA), a precursor that liberates 5-FU in human physiology and subsequently 5-FU in the lysosome. A sustained and site-specific release of PD is attributed to a higher efficacy of PD in killing U87 (IC<sub>50</sub>: ~20 µM for 48 h incubation), and SKOV-3 (with lower Est expression, IC<sub>50</sub>: ~36 µM for 48 h incubation) cancer cell lines, which are much lower than the IC<sub>50</sub> (≥ 50 µM) value for 5-FU in U87 cell line. Importantly, the cell viability for PD, when used in a much higher concentration (50 µM) in normal Chinese Hamster Ovary (CHO) cells, is evaluated as ~95%, which approves its probable efficacy in reducing systemic toxicity. The design of PD also enables us to achieve a 'TURN-ON' fluorescence response on



Est-mediated cleavage of the ester functionality and demonstrates its potential for theranostic applications. Flow cytometry studies reveal death for live U87 cancer cells in both early and late apoptotic regions. CAM assay also confirmed the superiority of PD in limiting the development of the blood vasculature of the embryonic membrane to signify their antiangiogenic behaviour. Therapeutic efficacy of the PD is also demonstrated in a spheroid model, developed using human cervical cancer (HeLa) cell multicellular tumour sphere culture.

## Introduction

5-Fluorouracil (5-FU), a pyrimidine analogue of DNA/RNA base and an antimetabolite, is the third most used chemotherapeutic agent in the treatment of solid malignancies across the world.<sup>1-4</sup> The market size for 5-FU was valued at \$2.45 billion in 2023, with an anticipated compound annual growth rate of 7.7% for the period 2024-2030.<sup>5</sup> However, 5-FU is also associated with severe cardiotoxicity, acute coronary syndrome, myocardial infarction, neurologic abnormalities and severe toxicity, even causing death in patients having dihydropyrimidine dehydrogenase deficiency.<sup>6,7</sup> It also enhances the risk of getting an infection due to compromised white blood cell counts. 5-FU has a narrow therapeutic index and is sparingly soluble in water. The plasma concentration of 5-FU is affected by numerous factors, thereby limiting its efficacy. A higher dose intensity of 5-FU is beneficial in improving the prognosis for treating gastrointestinal neoplasms—unfortunately, this also comes with dose-dependent toxicity.<sup>8</sup> It has been argued that efficacy could be improved through specific accumulation of 5-FU in the tumour-infected regions with sustained release.<sup>9,10</sup> Antibody-drug conjugates (ADCs) are one of the most popular choices for improving efficacy, as this allows site-specific drug release, improving effective local drug concentration at the tumour site, which helps in reducing drug doses and systemic toxicity of anticancer drugs.<sup>11,12</sup> An ADC of 5-FU is reported to preferentially target and inhibit HER2-expressing cancer cells. Research in ADCs is still in its infancy, and challenges like unfavourable pharmacokinetics, target-specific payload release, and off-target toxicity still limit the potential of different ADCs in clinical trials. Additionally, proteolytic cleavage could be an immune evasion mechanism for ADCs.<sup>13-15</sup> To address this, fully human monoclonal antibodies (mAbs) are used in recent ADCs. For most oncology mAbs, no clinically significant effect of binding or neutralising anti-drug antibodies in terms of pharmacokinetics.<sup>16</sup> Typically, non-human mAbs used in ADCs are large (~ 150 kDa), and this may limit their permeability to penetrate target tissues and cells.<sup>17, 18</sup> Very recently, Lan and coworkers have reported an ADC for 5-FU using a HER2-targeting protein, ZHER2:2891, fused with yeast cytosine deaminase (Fcy).<sup>18</sup> This needs extensive knowledge



in designing/purifying his6-tagged Fcy fusion proteins and expertise in chemical biology involving time-consuming, intricate methodologies.

Despite several successes of clinically approved ADCs for therapeutic applications, certain factors pose challenges to their optimal use, such as metabolic instabilities toward proteolytic enzymes, rapid clearance, protein aggregation, or high aggregation propensity in the formulation and drug resistance mechanisms.<sup>19-21</sup> ADCs target overexpressed antigens at the surface of cancer cells, and tumour-specific antigens are limited in human physiology. Importantly, some of these antigens are endogenously expressed in other normal tissues. These, along with an unfavourable drug: payload distribution in ADCs, an insufficient target in heterogeneous tumours, and poor tissue penetration in solid tumours, contribute to a  $\geq 1\%$  accumulation of the dosed ADCs. This accounts for the undesired nonspecific release and off-target toxicity.<sup>22</sup> To evade these limitations, the concept of prodrugs has been introduced. Prodrugs are derivatives with favourable physicochemical and pharmacokinetic properties compared to the parent active pharmaceutical ingredient (API) and undergo biochemical transformation within the human physiology in the presence of endogenous stimuli/stimulus to generate the API *in situ* to initiate the desired pharmacological effect.<sup>23-28</sup> Prodrugs with improved absorption, distribution, metabolism, and excretion (ADME) properties are safer and more efficacious alternatives to parent drug molecules. Further, the prodrug concept utilises the 505(b)(2) pathway to save significant time and expenses when an FDA-approved drug is being used for prodrug development.<sup>29,30</sup> Thus, such a strategy is beneficial from a regulatory standpoint as well. Notably, approximately 13% of the drugs approved by the U.S. Food and Drug Administration (FDA) between 2012 and 2022 were prodrugs.<sup>29-31</sup>

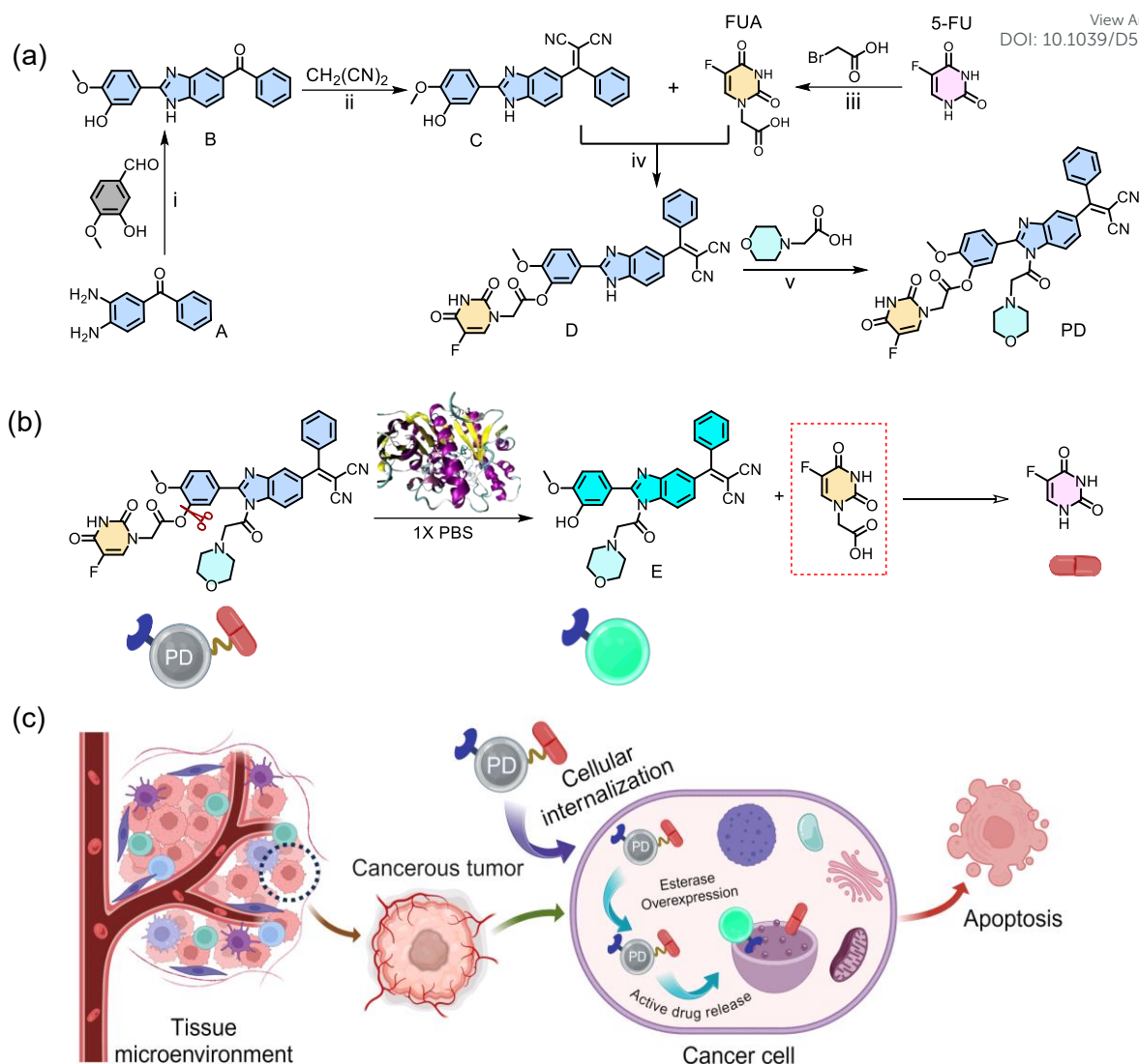
Barring one report on an ADC of 5-FU, there is no example in the contemporary literature to address the issue of the high systemic toxicity of one of the most prescribed chemotherapeutic drugs.<sup>32</sup> Whereas, there are several literature reports on using 5-FU as a probable active API, and it is proposed that 5-FU induces cell cycle arrest at the S phase and causes cell death primarily through apoptosis.<sup>33</sup> The most crucial requirement for creating a prodrug system is site-specific delivery of the drug.<sup>34,35</sup> Delivering the prodrug directly into certain organelles enables the drug to be accumulated at its intended location (the subcellular compartment), thereby minimising drug efflux and decreasing the likelihood of side effects, representing a promising approach for effective cancer treatment.<sup>36-39</sup> Inspired by this, we have reported a lysosome-targeted prodrug (PD) derived from 5-Fluorouracil-1-acetic acid (FUA) for targeted cancer therapy (Scheme 1a-c). FUA is a derivative of 5-FU and is known to undergo a



proteolytic degradation process in human blood plasma to yield 5-FU.<sup>40</sup> FUA is conjugated with a benzimidazole-based fragment as a luminescent marker and a morpholine moiety as a lysosome targeting fragment to synthesise PD. Importantly, our design allows the luminescent marker to remain in the 'OFF state' when conjugated with FUA. FUA is conjugated to the luminescent marker through an ester linkage that is susceptible to an enzymatic cleavage in the presence of esterase (Est), an enzyme that is typically overexpressed in various cancer cells such as glioblastoma (U87) cells, human ovarian cancer (SKOV-3) cells and human cervical cancer (HeLa) cells.<sup>41-45</sup> FUA is expected to get released inside the lysosome of the Est overexpressed cancer cells, along with morpholine conjugated benzimidazole (E), a derivative that exists in the luminescent 'ON state.' Thus, one would expect to monitor the luminescence ON response to probe the release/distribution of FUA in lysosomes of a cancer cell in the presence of endogenous stimuli like Est. FUA, as reported earlier, undergoes an enzymatic cleavage to release 5-FU, the active API.<sup>40,46-48</sup> Confocal Laser Scanning-Microscopy (CLSM) shows the higher cellular internalisation of PD compared to FUA and significant co-localisation with lysosome in the U87 cells. MTT assay studies reveal that such a site-specific drug release reduces the systemic toxicity of PD, apart from favouring crucial issues like sustained drug release and increased drug efficacy compared to 5-FU, FUA and the prodrug without lysosome targeting unit (D), where FUA is conjugated with a benzimidazole-based fragment. Thus, PD compliance with the 505(b)(2) regulatory pathway. PD is found to induce cell cycle arrest at the S phase and causes cell death primarily through apoptosis, having antiangiogenic behaviour and causes significant inhibition of the 3D spheroid growth of the HeLa cancer cells.

View Article Online  
DOI: 10.1039/D5SC03783B





**Scheme 1** (a) Molecular structures of 5-FU, FUA, PD, and all other intermediates used in synthesis and the synthetic scheme of PD: (i)  $\text{Na}_2\text{S}_2\text{O}_5$ , DMF,  $100^\circ\text{C}$ ; (ii)  $\text{NH}_4\text{OAc}$ , AcOH, Toluene; (iii) KOH, Water,  $50^\circ\text{C}$ ; (iv) EDC, HOBt, DMAP, DMF; (v) Oxalyl chloride, dry DCM and then DIPEA, DMF,  $0^\circ\text{C}$ . (b) Est-mediated drug release from PD. (c) Schematic representation of lysosome-targeted chemotherapeutic action and activation of PD inside the cancer cell (Created in BioRender. SARKAR, S. (2025) <https://BioRender.com/5ids1f7>).

## Results and discussion

The details of all synthetic methodologies adopted for the synthesis of PD, FUA, and all necessary intermediates are provided in the experimental section of the supporting information (ESI†). The prodrug, PD and all other intermediate compounds isolated during the synthesis processes were appropriately characterised using various analytical and spectroscopic techniques such as  $^1\text{H}$ -NMR,  $^{13}\text{C}$ -NMR and ESI-MS (Fig. S1-S15). All characterisation data for these intermediates and the final compound PD are discussed in the supporting information section (ESI†). Spectroscopic and analytical data ensured the desired purity of the PD and all





isolated intermediates. After successful synthesis, we performed the UV and luminescence spectroscopic analysis for PD (Fig. 1) and C (Fig. S16) to check the absorption and emission spectral pattern of both the fluorophore and the prodrug. All the spectroscopic measurements are done in 1X PBS buffer solution (pH 7.4). The absorption spectra recorded for PD and compound C reveal a broad absorption maximum at  $\sim 372$  nm ( $\epsilon$ : 17,400 M<sup>-1</sup> and 25,500 M<sup>-1</sup>, respectively) in 1X aq. PBS buffer medium (Fig. S16a). The emission spectra for PD and compound C were recorded in 1X aq. PBS buffer following excitation at 373 nm, and an insignificant emission spectrum was observed for PD, while a broad emission band having  $\lambda_{\text{em}}^{\text{Max}} \sim 430$  nm ( $\lambda_{\text{ext}} = 373$  nm) was observed for C (Fig. S16b). Presumably, this is attributed to an interruption of the intramolecular CT process in PD due to the presence of the ester functionality. As a result, the fluorescence is in an 'OFF' state in PD. Ester functionality in PD is expected to undergo a cleavage reaction in the presence of the Est. To examine this, we further performed the electronic and luminescence spectroscopic studies of PD after incubation with Est. A detectable change in the absorption spectrum of the PD (10  $\mu$ M, 1X PBS) was observed after incubation with 3 U/mL Est for 6 h (Fig. 1a inset), while a new and broad emission band appeared at  $\sim 505$  nm (Fig. 1a). Importantly, this emission spectrum of the cleaved product E after 6 h matched closely with the luminescence spectra for C (Scheme 1a), suggesting the effective cleavage of the ester functionality in PD induced by Est to yield E (Scheme 1b). Please note that both FUA, 5-FU and the morpholine moiety are non-luminescent. Intermediate compound D was also found to be practically non-luminescent as a result of interruption of the intramolecular CT process in D and PD due to the presence of the ester functionality (Fig. 1a). A plot of the change in luminescence intensity ( $[F_t - F_0]$ ), where  $F_t$  and  $F_0$  are the luminescence intensities at time  $t$  and  $t = 0$  respectively at 505 nm as a function of time revealed that the cleavage of the ester functionality and the release of the E (Fig. 1b), which is also synonymous with the release of FUA reached a plateau at  $\sim 6$  h. To further corroborate our presumption, we performed luminescence studies using varying concentrations of Est (0 to 5.2 U/mL at a successive gap of 0.5 U/mL and starting with 0.2 U/mL) in aq. PBS buffer medium (pH 7.4), maintaining a constant concentration of PD (10  $\mu$ M) (Fig. 1c). A clear dependency of the generation of E as a function of [Est] also validated our proposition (Scheme 1b and Fig. 1c). This was reconfirmed by recording the fluorescence spectra of compound D in the presence of increasing concentrations of Est under analogous experimental conditions as in the case of PD. The observed enhancement in fluorescence intensity with rising Est levels further validates our proposition (Fig. S17). We also examined the role of pH in inducing the



Est-mediated bond cleavages by monitoring the emission of the fragment E (due to the Est-mediated cleavage of PD) and compound C at different media pH and maintaining other reaction conditions unchanged. A higher emission intensity for E at a lower pH suggests a more effective release of FUA at a lower pH (Fig. S18a-b). This also suggests a slow and sustained release of FUA and then 5-FU in physiological conditions (1X aq. PBS buffer, pH 7.4). Earlier reports suggest FUA undergoes intracellular metabolic transformation to yield 5-FU.<sup>40,46-48</sup> Higher glucose metabolism in the cancer tissue/cells leads to an enhanced  $H^+$  production. Additionally, poor perfusion in malignant tumours results in an acidic extracellular pH (6.5 – 6.9) compared to normal tissue under physiologic conditions (7.2 – 7.4).<sup>49,50</sup> Thus, the release of FUA from PD is expected to be further favoured in malignant tumours.

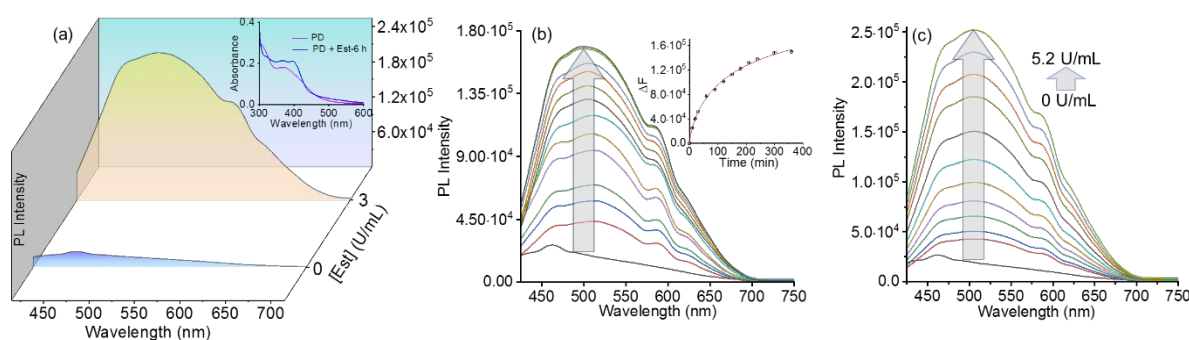


**Fig. 1** (a) Emission spectra of PD (10  $\mu$ M) in the absence and presence of the enzyme Est are recorded in phosphate buffer (pH 7.4), showing the fluorescence activation upon Est treatment and absorption spectra in the inset. (b) The time-dependent release of E from PD upon Est treatment is recorded for 0, 0.5, 1, 1.5, 2, 2.5, 3, 3.5, 4, 5, and 6 h. The change in fluorescence intensity  $\Delta F$  ( $F_t - F_0$ ) as a function of time for 6 h is shown in the inset. (c) A consistent increase in fluorescence intensity in an Est concentration-dependent drug release study from 0 to 5.2 U/mL by starting the titration with 0.2 U/mL and then at a successive gap of 0.5 U/mL.

To confirm the specificity of this cleavage reaction towards Est, control experiments were performed by treating the 10  $\mu$ M PD with 1 mM concentrations of various bioanalytes (Cys, Hcy, Arg, Trp, Asn, Met, Gly, Pro, His, GSH, Phe, Ile, Asp, Glu, Lys, Leu, Est). The absence of any detectable increase in luminescence intensity confirmed the specificity of the biochemical transformation involving PD and Est (Fig. S19). Further, the Est-induced release of FUA from PD was examined using reverse-phase high-performance liquid chromatography (RP-HPLC). RP-HPLC profiles for pre-synthesized and characterised PD, FUA, and intermediate C were recorded (Fig. 2). We used an analogous compound C as a reference to understand the possible retention time for E that was produced *in situ* from Est-treated PD. RP-





HPLC was performed for 50  $\mu$ M solutions of each of PD, FUA, C, and PD incubated with Est (5 U/mL) at different time intervals (2, 4, and 6 h) using acetonitrile/water (1:1) as eluent and performed isocratically. The detailed procedure and the experimental conditions are described in the ESI.† Retention times for different pre-synthesised species are as follows:  $t_{PD}$ : 5.93 min;  $t_{FUA}$ : 2.8 min;  $t_C$ : 6.98 min (Fig. 2). On incubation of PD with Est, two new peaks appeared with a retention time of 6.63 min and 2.8 min. Both peaks were found to increase with increasing incubation time (0 - 6 h). The new peak with a retention time of 6.63 min was relatively close to the retention time for C ( $t_C$ : 6.98 min) and was assigned to the fragment E (Scheme 1b). The slightly lower retention time for E as compared to C can be rationalised based on the presence of a lysosome-targeting, more polar morpholine group in E. The other peak at 2.8 min appeared at the same place as for FUA and confirmed its release through the enzymatic cleavage of PD. Thus, RP-HPLC studies confirmed the release of FUA and E on the enzymatic cleavage of PD induced by Est.

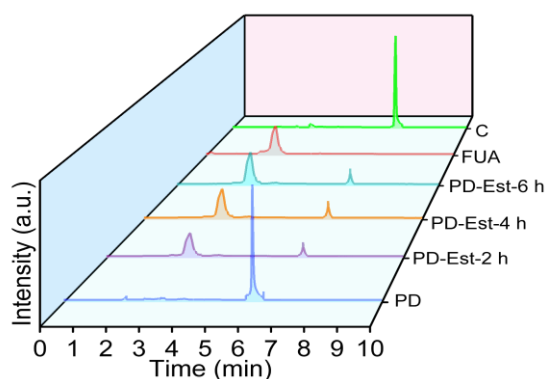


**Fig. 2:** RP-HPLC spectrum profile for PD, C, FUA, and Est-treated PD (50 $\mu$ M each) after 2, 4, and 6 h in 1X PBS buffer solution.

After ensuring the Est-mediated in-vitro release of FUA, which undergoes further metabolic processes to release 5-FU at the cancer tissue/cells,<sup>40,46-48</sup> along with the lysosome-targeted luminescence marker E, we further examined the cellular internalisation of PD in the U87 cancer cell line using CLSM. The overexpression of Est in cancer cell lines such as U87 is linked to increased cell proliferation and invasion.<sup>51-53</sup> The cellular uptake studies of the PD were carried out using U87 cell lines through CLSM (Fig. 3a-d). A green fluorescence was observed (indicated by a white arrow) in U87 cells, incubated with the PD for 24 h. This was rationalised as the intrinsic luminescence of the fragment E, generated through enzymatic cleavage induced by endogenous Est overexpressed in tumour cells (Fig. 3d and S20a). Est activity in malignant colorectal tumours ( $0.45 \pm 0.25$  U/L for males and  $0.45 \pm 0.35$  U/L for females) is much higher than in normal tissues ( $0.17 \pm 0.09$  U/L for males and  $0.12 \pm 0.07$  U/L



for females).<sup>54</sup> Reports suggest that stored fats in malignant tumours are released and support Est-induced cancer pathogenesis.<sup>55,56</sup> We have earlier established that the release of E is also associated with the release of an equimolar amount of FUA. Incubation with either FUA or C, used in identical concentrations as PD, failed to show any similar uptake (Fig. 3b-c). The confocal microscopic images are quantified using IMAGEJ software and presented in Fig. S20b, which also supports the above results. The terminal-COOH functionality in FUA remains as a carboxylate and fails to diffuse through the lipid core of the plasma membrane. This accounts for a lower cell membrane permeability and reported cytotoxicity of FUA toward different cancer cells (A431, HT29, and HeLa cells) compared to 5-FU.<sup>57-59</sup> Thus, ester functionality in PD, as evident in CLSM images (Fig. 3a-d), helps in improving the cellular permeabilisation of FUA.

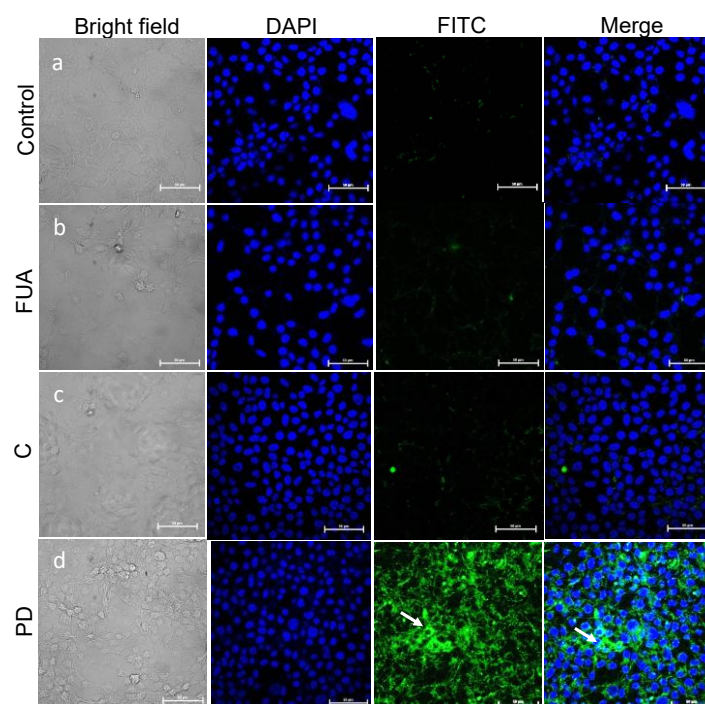


**Fig. 3** Representative images of cellular uptake of our designed prodrug and respective control molecules in U87 cells (a) control, (b) FUA (10  $\mu$ M), (c) C (10  $\mu$ M), and (d) PD (10  $\mu$ M); where Column I: Bright field, II: DAPI, III: FITC, IV: Merge images. The images were acquired using confocal microscopy (laser used DAPI: 404.2, PD/C/FUA: 535 nm, green) at 60x magnification, scale bar = 50  $\mu$ m.

Following this, we checked for colocalization of PD in mitochondria/lysosomes using mito-tracker red/lyso-tracker red through CLSM studies. The U87 cells were treated with FUA, C, and PD for 24 h, followed by incubation with mito-/lyso-tracker red for 15-20 min before the termination of the experiment to stain the subcellular organelles, mitochondria/lysosomes. Results of the intracellular co-localisation of PD with U87 cells are presented in Fig. S21 and



4a-c. Results reveal that when U87 cells are incubated with PD, individual green and red fluorescence (for *in situ* release of E) was observed in the FITC (for uptake of the prodrug molecule) and Cy5 channels (for mitochondria/lysosome staining), respectively. The green fluorescence in the FITC channel further confirms the release of FUA and eventually 5-FU in malignant tumours through the enzymatic cleavage of the ester functionality in PD by endogenous Est. The merged image of FITC channel with Cy5 indicates that PD molecules, even though internalised into the cell, but not localised in the subcellular organelle mitochondria (individual green and red fluorescence: Fig.S21c), but it is localised in the lysosome (yellow fluorescence due to merging of red and green: Fig. 4c). Thus, CLSM images of the colocalization studies with lysotracker red/mitotracker red confirm that the release of E happens in lysosomes, not in mitochondria. The localisation of E in the lysosome also ensures the localisation of PD in the lysosome. Lysosomes typically maintain a highly acidic environment (pH  $\sim$  4.5-5.0), which favours the localisation of morpholine functionality present in E and PD. Also, no fluorescence within the lysosome was observed for other control molecules, FUA and C (Fig. 4a-b). This confirmed the design philosophy for developing the purpose-built prodrug PD and its effective release in the lysosome for better therapeutic efficacy.

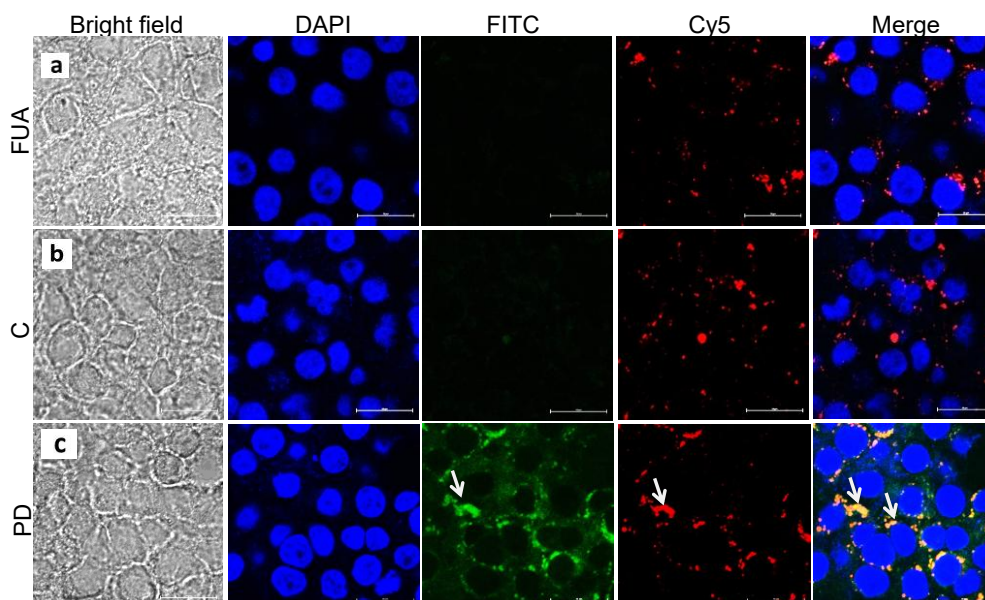


**Fig. 4** Representative images of lysosomal internalisation of our designed prodrug (PD) and respective control molecules (FUA and C) in U87 cells using lyso-tracker red (a) FUA (10  $\mu$ M), (b) C (10  $\mu$ M), and (c) PD (10  $\mu$ M); where Column I: Bright field, II: DAPI, III: FITC, IV: Cy5, V: Merge images. The images were acquired in confocal microscopy (laser used for DAPI: 404.2 nm, PD/FUA/C: 535 nm (green), and lysotracker: 595 nm (red) at 60x magnification, scale bar = 50  $\mu$ m.



We further examined the cell viability of FUA, 5-FU, PD, and C towards various cancer cell lines (U87, SKOV-3) using MTT assay in a dose-dependent (1-100  $\mu$ M) time dependent (48 h and 72 h) manner, and compared the cytotoxicity results with normal Chinese Hamster Ovary (CHO) cell lines. It is evident from Fig. S22 that CHO cells, incubated with PD/FUA/C, show insignificant toxicity after 48h incubation even at a higher concentration (50 $\mu$ M). Further, the cytotoxic properties of PD, FUA, 5-FU and C were evaluated in different cancer cell lines (U87 and SKOV-3; Fig. 5a-d) following incubation over a varying time. Results revealed that PD adversely affected the cancer cell viability in a dose (1-100  $\mu$ M) and time-dependent manner (48 and 72 h) and was more cytotoxic towards cancer cell lines as compared to other precursor compounds (FUA and C). Even the actual drug 5-FU shows lesser toxicity as compared to PD. Table S1 summarises the IC<sub>50</sub> value of PD and other control molecules in U87 and SK-OV-3 cell lines. Importantly, PD induced higher toxicity towards U87 cell lines at lower concentrations, with an IC<sub>50</sub> value of 20.77 and 16.95  $\mu$ M on incubation for 48 and 72 h, respectively. The IC<sub>50</sub> values of PD in SK-OV-3 cells were found to be 36.85 and 32.47  $\mu$ M, respectively, on incubation for 48 and 72 h. Also, PD is found to be more toxic than naked 5-FU, which shows higher toxicity than FUA but less toxicity than PD in both U87 and SKOV-3 cell lines. To further investigate the lysosome-targeting effect, we evaluated the cytotoxicity of compound D in U87 cancer cells and CHO normal cells over a 48h incubation period. Compound D exhibited negligible toxicity toward CHO cells at concentrations up to 50  $\mu$ M, while demonstrating a moderate cytotoxic effect in U87 cells, with an IC<sub>50</sub> value of 80.5  $\mu$ M after 48 h of treatment (Fig. S22 and S23). These studies confirmed that PD is also more toxic than D, and this essentially confirms the role of lysosome-specificity of PD as compared to D. This demonstrates the importance of the specificity of PD towards lysosomes, which subsequently causes higher toxicity owing to a higher local concentration of PD inside the cancer cell organelle. Since PD is more cytotoxic towards U87 cell lines, other *in vitro* experiments are carried out in this cell line using a 10  $\mu$ M concentration (lower than the IC<sub>50</sub> value). Presumably, a higher expression of Est enzymes in the U87 cell line compared to other cell lines accounts for the higher toxicity of PD.<sup>41,42</sup> The observed toxicity of PD towards U87



cells further corroborates the observations of the earlier researchers that FUA undergoes intracellular biochemical transformation to generate 5-FU.<sup>40,46-48</sup>

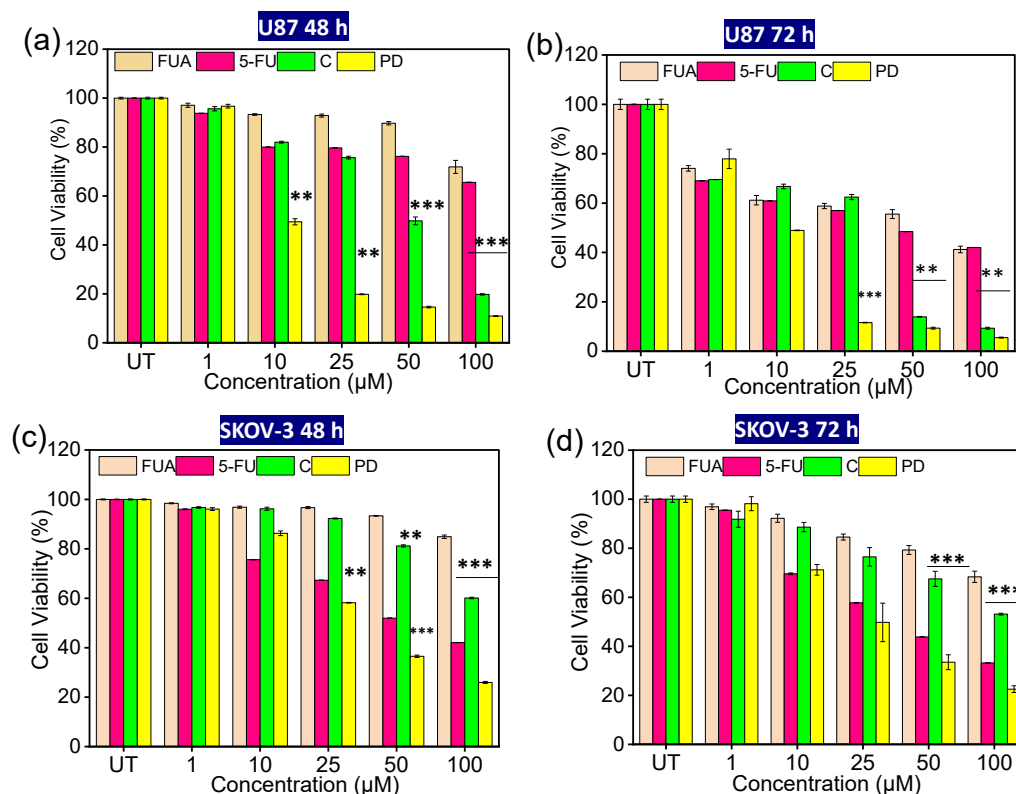


**Fig. 5** Cell viability assay in several cancer cell lines, such as (a-b) U87, and (c-d) SKOV-3. Our designed prodrug and respective control molecules (PD, FUA, 5-FU, and C) show a decrease the cancer cell viability in a dose (1-100 μM) and time (48 and 72 h) dependent manner. These experiments were performed in triplicate and represented as mean ± SD. Significant differences from untreated cells were observed at (\*p < 0.05, \*\*p < 0.01, \*\*\*p < 0.001).

An anticancer drug can inhibit cancer cell proliferation at different phases (sub-G1, G0-G1, S, and G2/M). To check the arrested phase in U87 cells in response to FUA, C, and PD (10 μM each), cell cycle analyses were carried out using flow cytometry after staining the cells with PI mix (Fig. 6a i-v). Several reports demonstrate that 5-FU arrests the cancer cell proliferation primarily at the S phase, apart from the G2/M phase.<sup>32</sup> For PD, cell cycle arrest for U87 cells happens at the S phase and also to some extent in G2/M phase, potentiating their cell death-inducing property (Fig. 6a-iv). However, for FUA and C, no significant cell cycle arrest (Fig. 6a-i-iii) was observed. The % of cell populations for all flow cytometry data were analysed and is presented in Fig. 6a-v.





The cell death process was studied using FACS (Fluorescence-Activated Cell Sorting) studies to understand the programmed cell death-inducing potential of PD toward U87 cell lines (Fig. 6b i-v). For this, U87 cells were incubated with Annexin V/FITC and PI, and the % of cells in different phases was investigated through flow cytometry. In the early phases of apoptosis, annexin V preferentially binds to phosphatidylserine that is visible on the plasma membrane's outer leaflet. On the other hand, PI is a DNA intercalating agent that penetrates late apoptotic and necrotic cells but is excluded from viable cells with intact membranes. Q1 (FITC-/PI+), Q2 (FITC+/PI+), Q3 (FITC-/PI-), and Q4 (FITC+/PI-) quadrants represent necrotic, late apoptotic, healthy and early apoptotic cell populations, respectively. Results reveal that, in response to the PD, % of the U87 cell population is higher in both early and late apoptotic regions as compared to other precursor molecules (FUA and C) and the untreated control group, which is also supported by an earlier report.<sup>60</sup> Percentage (%) of the cell population at different phases was also analysed and graphically presented in Fig. 6b-v. The results altogether indicate the apoptosis-inducing properties of PD molecules towards U87 cells.

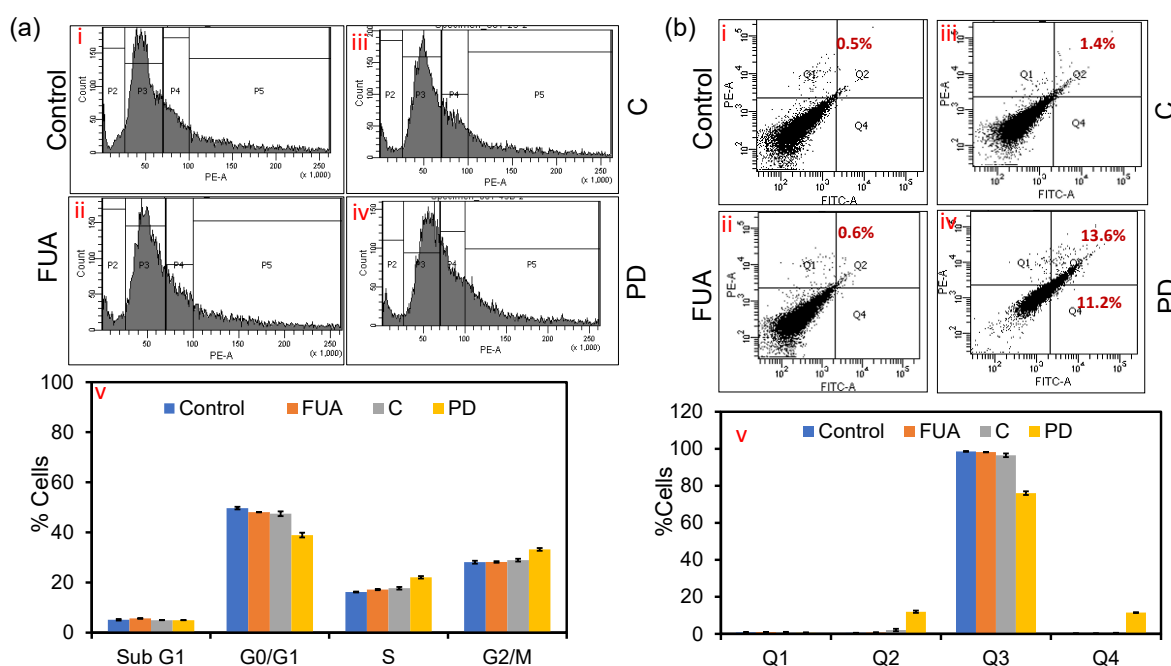


**Fig. 6** Cell cycle and apoptosis analysis were done in U87 cells, where in Panel I (cell cycle analysis): (a) (i) control, (ii) FUA, (iii) C, (iv) PD, and (v) graphical presentation of % cells in different phases of the cell cycle. The prodrug molecule PD arrests the U87 cells in the S and G2/M phases. Panel II (Apoptosis analysis): (b) (i) control, (ii) FUA, (iii) C, (iv) PD, and (v) graphical presentation of % cells in different apoptotic phases. The prodrug molecule PD exhibits both early and late apoptotic cell death. Three independent experiments are performed and represented as mean  $\pm$  SD.





We further performed a chick embryo chorioallantoic membrane (CAM) assay to check the antiangiogenic properties of PD. CAM possesses an extensive capillary network expressing Fibroblast growth factor 2 that limits the development of the vascular system of the embryonic membrane.<sup>61, 62</sup> CAM assay is a simple *in vivo* model to study the effect of new drugs on the extraembryonic membrane of the developing chick embryo. We performed the CAM assay to study the effect of PD, C, and FUA on the extraembryonic membrane of developing chick embryos. The results are presented in Fig. 7. A narrow hole was created on the fertilized eggs on day 4 and the chorioallantoic membrane was incubated with our designed prodrug (PD) and respective control molecules (FUA and C) 100  $\mu$ M each for 4 h. Results revealed that, there was a slight disruption of blood vasculature upon FUA and C incubation. However, a significant inhibition of blood vasculature was observed when the chorioallantoic membrane was incubated with the prodrug molecules (PD) exhibiting their antiangiogenic property. The blood vessel diameter was quantified to reveal the % of fold change using ImageJ software and represented in Fig. S24 and Table S2, which also matched well with the above observation. This further confirmed the efficacy of PD as a stimulus-responsive organelle-specific anti-cancer drug.

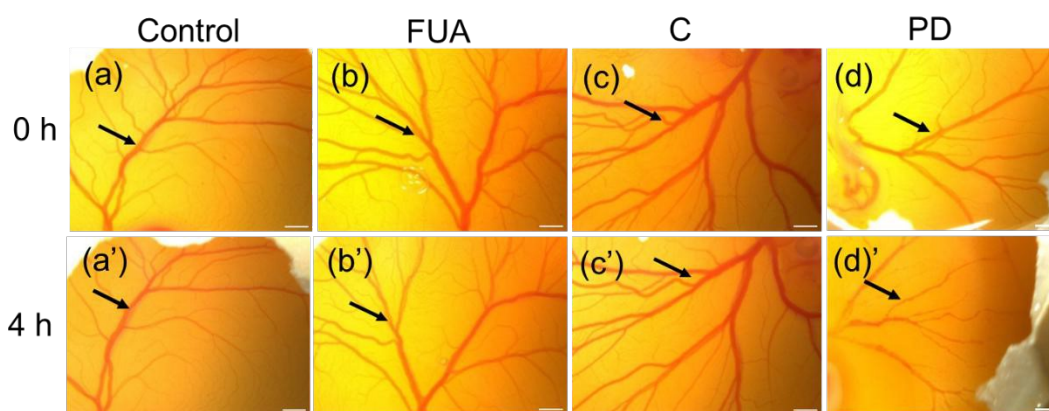


**Fig. 7** Chorioallantoic membrane assay. Representative CAM images at 0 and 4 h, where (a-a') control, (b-b') FUA, (c-c') C, and (d-d') PD. The blood vessels of the chick embryo are more inhibited in response to the PD molecules (indicated by black arrows), potentiating the anti-angiogenic potential of the pro-drug molecules. Images were taken using a Leica stereo microscope at 1x magnification, scale bar = 5 mm.

Finally, we have investigated the effectiveness of PD and FUA in 3D multicellular tumour spheroids. HeLa cell multicellular tumour sphere culture (MCTS) in three dimensions was developed in our lab following the previously described 3D sphere creation for tumour mimicking.<sup>63</sup> Spheroid models are considered a close representation of *in vivo* models.<sup>64</sup> A significant decrease in the size of the spheroids was observed for the PD (50  $\mu$ M) treated group



compared to the group treated with FUA (50  $\mu$ M; Fig. 8). An increase in the size of the spheroids was observed in the control group. This data further validates the higher efficacy of the PD compared to that of FUA in inhibiting spheroid growth, which closely mimics the main features of human solid tumours.

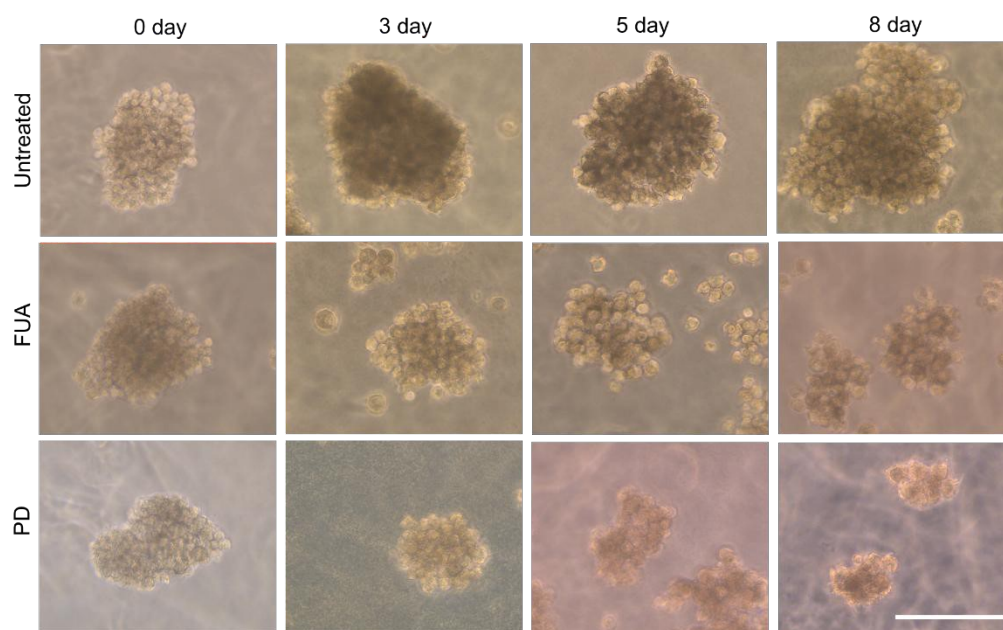


**Fig. 8** The bright field images indicate the size of the spheroid on the indicated day after FUA and PD treatment, along with the control. The size is significantly decreased in both the FUA and PD-treated groups, and PD has better efficacy compared to FUA. The scale bar corresponds to 100  $\mu$ m.

## Conclusion

5-FU is an anti-metabolite that interferes with the synthesis and function of DNA and RNA in cancer cells by inhibiting thymidylate synthase in malignant and non-malignant cells, which induces severe systemic toxicity. A new lysosome-targeted prodrug (PD) is synthesised to address the issue of high systemic toxicity by enhancing the efficacy through sustained release of 5-FU specifically in lysosomes through functionalization with morpholine. Further, it is demonstrated that by leveraging the overexpression of Est enzymes in human glioblastoma (U87) cells, site-specific, sustained, and sequential release of the FUA and 5-FU in the lysosome is achieved. It is not unreasonable to link these to the higher efficacy of PD in killing U87 and SKOV-3 cancer cell lines. The design of PD enabled us to realise a 'TURN-ON' fluorescence response upon Est-mediated cleavage of the ester functionality and confirms its potential for theranostic applications. IC<sub>50</sub> values for PD for U87 and SKOV-3 cells are found



to be 20.77 and 36.85  $\mu\text{M}$ , respectively, on incubation for 48h. While  $\text{IC}_{50}$  values for 5-FU in U87 and SKOV-3 cells are  $\sim 105$  and 48  $\mu\text{M}$ , respectively, under identical experimental conditions. Importantly, the cell viability for PD, when used in a much higher concentration (50  $\mu\text{M}$ ) in normal healthy CHO cells, is evaluated as  $\sim 95\%$ , which approves its probable efficacy in reducing systemic toxicity. Flow cytometry studies in U87 cells confirm that PD causes both early and late apoptotic death as compared to other precursor molecules (FUA and C) and the untreated control group. Importantly, the CAM assay confirmed the superiority of PD in limiting the development of the blood vasculature of the embryonic membrane to signify its antiangiogenic behaviour. Efficacy is also demonstrated in a 3D spheroid model developed using HeLa cell multicellular tumour sphere culture. A significant decrease in the size of the spheroids was observed for the PD (50  $\mu\text{M}$ ) treated group compared to the group treated with FUA (50  $\mu\text{M}$ ).

### Data availability

The data supporting this article have been included as part of the Supplementary Information (ESI<sup>†</sup>).

### Authors Contributions

Sourav Dutta: Scholar associated with synthesis, scale up synthesis, characterization, photochemical and physicochemical studies, and manuscript preparation. Sanchita Tripathy: Scholar associated with in vitro cell culture and angiogenesis studies. Somnath Bej: associated partly with synthesis, and photochemical studies. Sabana Parvin: associated partly with synthesis and characterization, Batakrishna Jana: biological studies, interpretation and correlation of the data, and writing of this article. Chitta Ranjan Patra: Overall supervision of intracellular and angiogenesis studies, interpretation and correlation of the biological data and writing of this article. Amitava Das: Conceptualization, overall supervision, interpretation and data correlation, overall coordination, and writing of the article.

### Conflicts of Interest

The authors declare no conflicts of interest.

### Acknowledgement

A.D. acknowledges the ANRF-J.C. Bose Fellowship and funding through the JBR/2023/000005 grant. A.D. also acknowledges the MoE-STARS research grant (No. 2023-47) for financial support. S.D. acknowledges IISER Kolkata for the Senior Research



Fellowship (SRF). S.B. acknowledges the ANRF Postdoctoral fellowship award (PDF/2023/003483) for financial support. BJ acknowledges the ANRF-Ramanujan Fellowship (RJF/2022/000127) for support. CRP is thankful to DST, New Delhi (CRG/2022/004594: GAP0985) for partial financial support for this research. ST is grateful to UGC for her Research Fellowship. CRP and ST thank the Director, CSIR-IICT (Ms. No IICT/Pubs./2025/177 dated May 13, 2025) for providing all the required facilities to carry out the work.

## References

1. J. D. Sara, J. Kaur, R. Khodadadi, M. Rehman, R. Lobo, S. Chakrabarti, J. Herrmann, A. Lerman, and A. Grothey, *Ther. Adv. Med. Oncol.*, 2018, **10**.
2. D. B. Longley, D. P. Harkin and P. G. Johnston, *Nat. Rev. Cancer*, 2003, **3**, 330-338.
3. K. Miura, M. Kinouchi, K. Ishida, W. Fujibuchi, T. Naitoh, H. Ogawa, T. Ando, N. Yazaki, K. Watanabe, S. Haneda, C. Shibata, and I. Sasaki, *Cancers*, 2010, **2**, 1717-1730.
4. J.-K. Chen, K. A. Merrick, Y. W. Kong, A. I. -Tomasevic, G. Eng, E. D. Handly, J. C. Patterson, I. G. Cannell, L. S. -Lopez, A. M. Hosios, A. Dinh, D. S. Kirkpatrick, K. Yu, C. M. Rose, J. M. Hernandez, H. Hwangbo, A. C. Palmer, M. G. V. Heiden, Ö. H. Yilmaz, M. B. Yaffe, *Cell Rep. Med.*, 2024, **5**, 101778.
5. Global Fluorouracil (5FU) Market Size By Type, By Route Of Administration, By Geographic Scope And Forecast;  
[https://www.verifiedmarketresearch.com/product/fluorouracil-5fu-market/#:~:text=Fluorouracil%20\(5FU\)%20Market%20was%20valued,7.7%25%20from%202024%20to%202030](https://www.verifiedmarketresearch.com/product/fluorouracil-5fu-market/#:~:text=Fluorouracil%20(5FU)%20Market%20was%20valued,7.7%25%20from%202024%20to%202030), access date 20/05/2025.
6. C. Yuan, H. Parekh, C. Allegra, T. J. George, and J. S. Starr, *Cardio-Oncology*, 2019, **5**, 13.
7. J. Latchman, A. Guastella, C. Tofthagen, *Clin. J. Oncol. Nurs.* 2014, **18**, 581-585.
8. J. J. Lee, J H. Beumer, E. Chu, *Cancer Chemother Pharmacol*, 2016, **78**, 447–464.
9. G. Huang, Y. Xie, Z. Jiang, Z. Xu, Z. Jin, K. Xu, *Curr. Probl. Surg.*, 2025, **66**, 101746.
10. P. M. Wallace, J. F. MacMaster, V. F. Smith, D. E. Kerr, P. D. Senter, W. L. Cosand, *Cancer Res*, 1994, **54**, 2719–2723.
11. A. Thomas, B. A. Teicher, and R. Hassan, *Lancet Oncol.*, 2016, **17**, e254–e262.
12. Z. Fu, S. Li, S. Han, C. Shi, and Y. Zhang, *Sig Transduct Target Ther*, 2022, **7**, 93.
13. T. Miyoshi-Akiyama, I. Ishida, M. Fukushi, K. Yamaguchi, Y. Matsuoka, T. Ishihara, M. Tsukahara, S. Hatakeyama, N. Itoh, A. Morisawa, Y. Yoshinaka, N. Yamamoto, Z. Lianfeng, Q. Chuan, T. Kirikae and T. Sasazuki, *J. Infect. Dis.*, 2011, **203**, 1574-1581.



14. M. G. Romei, B. Leonard, I. Kim, H. S. Kim, and G. A. Lazar, *J. Biol. Chem.*, 2023, **299**, 104685. View Article Online  
DOI: 10.1039/D3SC03783B
15. D. M. H. Van Rijswijck, A. Bondt, N. De Kat, R. Lood and A. J. R. Heck, *Anal. Chem.*, 2024, **96**, 23–27.
16. M. Grairi, M. L. Borgne, *Drug Discov. Today*, 2024, **29**, 104241.
17. Global Antibody-drug Conjugates Market. Strategic Market Research Website. <https://www.strategicmarketresearch.com/market-report/antibody-drugconjugates-market>. Published June 2022. Accessed October 10, 2024.
18. K-H. Lan, C-L. Tsai, Y-Y. Chen, T-L. Lee, C-W. Pai, Y. Chao, K-L. Lan, *Biochem. Biophys. Res. Commun.*, 2021, **582**, 137-143.
19. C. McKertish and V. Kayser, *Biomedicines*, 2021, **9**, 872.
20. K. Tsuchikama and Z. An, *Protein & Cell*, 2018, **9**, 33–46.
21. H. Gao, Z. Xi, J. Dai, J. Xue, X. Guan, L. Zhao, Z. Chen, and F. Xing, *Mol Cancer*, 2024, **23**, 88.
22. H. E. Marei, C. Cenciarelli, and A. Hasan, *Cancer Cell Int*, 2022, **22**, 255.
23. Y. Wang, D. Xiao, J. Li, S. Fan, F. Xie, W. Zhong, X. Zhou and S. Li, *Sig Transduct Target Ther*, 2022, **7**, 20.
24. J. B. Zawilska, J. Wojcieszak, A. B. Olejniczak, *Pharmacol. Rep.*, 2013, **65**, 1-14.
25. M. Markovic, S. Ben-Shabat, and A. Dahan, *Pharmaceutics*, 2020, **12**, 1031.
26. X. Xie, T. Yu, X. Li, N. Zhang, L. J. Foster, C. Peng, W. Huang, and G. He, *Sig Transduct Target Ther*, 2023, **8**, 335.
27. A. Husain, J. Monga, S. Narwal, G. Singh, M. Rashid, O. Afzal, A. Alatawi and N. M. Almadani, *Chem. Biodiversity*, 2023, **20**, e202301169.
28. M. A. M. Subbaiah, J. Rautio and N. A. Meanwell, *Chem. Soc. Rev.*, 2024, **53**, 2099–2210.
29. W. F. Salminen, O. Aloba, A. Drew, A. Marcinowicz, M. Huang, *Drug Discov. Today*, 2023, **28**, 103618.
30. W. F. Salminen, M. E. Wiles, R. E. Stevens, *Drug Discov. Today*, 2019, **24**, 46-56.
31. M. M. De Souza, A. L. R. Gini, J. A. Moura, C. B. Scarim, C. M. Chin and J. L. Dos Santos, *Pharmaceutics*, 2025, **18**, 297.
32. P. M. De Angelis, D. H. Svendsrud, K. L. Kravik and T. Stokke, *Mol Cancer*, 2006, **5**, 20.
33. J. Rautio, N. A. Meanwell, L. Di, and M. J. Hageman, *Nat. Rev. Drug Discov.*, 2018, **17**, 559–587.
34. R. Walther, J. Rautio, A. N. Zelikin, *Adv. Drug Deliv. Rev.*, 2017, **118**, 65-77.





35. W. Chen, G. Luo and X. Zhang, *Adv. Mater.*, 2019, **31**, 1802725.
36. H. Padh and Niraj Sakhrani, *Drug Des. Devel. Ther.*, 2013, **7**, 585-599.
37. H. He, J. Wang, H. Wang, N. Zhou, D. Yang, D. R. Green and B. Xu, *J. Am. Chem. Soc.*, 2018, **140**, 4, 1215–1218.
38. B. Jana, S. Jin, E. M. Go, Y. Cho, D. Kim, S. Kim, S. K. Kwak, J. -H, *J. Am. Chem. Soc.*, 2023, **145**, 18414-18431.
39. L. Yang, R. Peltier, M. Zhang, D. Song, H. Huang, G. Chen, Y. Chen, F. Zhou, Q. Hao, L. Bian, M-L. He, Z. Wang, Y. Hu, H. Sun, *J. Am. Chem. Soc.*, 2020, **142**, 18150–18159.
40. Q. Luo, P. Wang, Y. Miao, H. He, X. Tang, *Carbohydr. Polym.*, 2012, **87**, 2642-2647.
41. Z. Ye, L. Gao, J. Y. Cai, Y. X. Wang, Y. Li, S. A. Tong, T. F. Yan, Q. Sun, Y. Z. Qi, Y. Xu, H. Jiang, S. Zhang, L. Zhao, S. Zhang, & Q Chen, *Nanomedicine: Nanotechnology, Biology and Medicine*, 2022, **44**, 102581.
42. Y. Y. Ma, W. J. Gao, S. H. Ma, Y. Y. Liu, W. Y. Lin, *Anal Chem*, 2020, **92**, 13405-13410.
43. N. Qiu, X. Liu, Y. Zhong, Z. Zhou, Y. Piao, L. Miao, Q. Zhang, J. Tang, L. Huang and Y. Shen, *Adv. Mater.*, 2016, **28**, 10613–10622.
44. Z. Zhou, W. J. Murdoch, Y. Shen, *J. Polym. Sci., Part A: Polym. Chem.*, 2016, **54**, 507-515.
45. Y. Z. Yang, Z. Y. Xu, N. B. Li, H. Q. Luo, *Spectrochim. Acta A Mol. Biomol. Spectrosc.*, 2021, **262**, 120094.
46. Y. Sun, J. A. Kaplan, A. Shieh, H.-L. Sun, C. M. Croce, M. W. Grinstaff, and J. R. Parquette, *Chem. Commun.*, 2016, **52**, 5254–5257.
47. V. Ciaffaglione, M. N. Modica, V. Pittalà, G. Romeo, L. Salerno, S. Intagliata; *ChemMedChem*, 2021, **16**, 3496-3512.
48. P. Chakraborty and P. Dastidar, *Chem. Commun.*, 2019, **55**, 7683–7686.
49. V. Estrella, T. Chen, M. Lloyd, J. Wojtkowiak, H. H. Cornnell, A. Ibrahim-Hashim, K. Bailey, Y. Balagurunathan, J. M. Rothberg, B. F. Sloane, J. Johnson, R. A. Gatenby and R. J. Gillies, *Cancer Res*, 2013, **73**, 1524–1535.
50. I. Böhme and A. K. Bosserhoff, *Pigment Cell Melanoma Res.*, 2016, **29**, 508–523.
51. B. Nowak, P. Rogujski, M. Janowski, B. Lukomska, A. Andrzejewska, *BBA - Reviews on Cancer*, 2021, **1876**, 188582.
52. A. Wlodarczyk, D. Grot, E. Stoczynska-Fidelus and P. Rieske, *Journal of Oncology*, 2020, **2020**, 6783627.
53. A. K. Madikonda, A. Ajayakumar, S. Nadendla, J. Banothu, V. Muripiti, *Bioorg. Med. Chem.*, 2024, **116**, 118001.
54. H. Dong, L. Pang, H. Cong, Y. Shen and B. Yu, *Drug Deliv*, 2019, **26**, 416-432.





55. H. Qin and Z.-H. Ruan, *Cell Biochem Biophys*, 2014, **70**, 33-36.
56. D. K. Nomura, J. Z. Long, S. Niessen, H. S. Hoover, S.-W. Ng and B. F. Cravatt, *Cell*, 2010, **140**, 49–61.
57. B. K. Gan, K. Rullah, C. Y. Yong, K. L. Ho, A. R. Omar, N. B. Alitheen, and W. S. Tan, *Sci Rep*, 2020, **10**, 16867.
58. R M Wohllhueter, R S McIvor, P G Plagemann, *J. Cell. Physiol.*, 1980, **104**, 309-319.
59. Sauraj, S. U Kumar, P. Gopinath, Y S Negi, *Carbohydrate Polymers*, 2017, **157**, 1442-1450.
60. U. Fischer, S. Steffens, S. Frank, N. G. Rainov, K. Schulze-Osthoff and C. M. Kramm, *Oncogene*, 2005, **24**, 1231–1243.
61. S. Javerzat, P. Auguste, A. Bikfalvi, *Trends Mol. Med.*, 2002, **8**, 483-489.
62. T. Jia, T. Jacquet, F. Dalonneau, P. Coudert, E. Vaganay, C. E. -Héritier, J. Vollaie, V. Josserand, F. Ruggiero, J. -L. Coll, B. Eymin, *BMC Biol.*, 2021, **19**, 173.
63. L. Wang, H. Guo, C. Lin, L. Yang and X. Wang, *Mol. Med. Rep.*, 2014, **9**, 2117–2123.
64. A. S. Nunes, A. S. Barros, E. C. Costa, A. F. Moreira and I. J. Correia, *Biotechnology and Bioengineering*, 2019, **116**, 206–226.

View Article Online  
DOI: 10.1039/D5SC03783B



## Data availability

View Article Online  
DOI: 10.1039/D5SC03783B

The data supporting this article have been included as part of the Supplementary Information (ESI<sup>†</sup>).

